

Heterogeneous & Homogeneous & Bio-

CHEM **CAT** CHEM

CATALYSIS

Supporting Information

© Copyright Wiley-VCH Verlag GmbH & Co. KGaA, 69451 Weinheim, 2014

Water-Promoted Hydrogenation of Levulinic Acid to γ -Valerolactone on Supported Ruthenium Catalyst

Jingjing Tan,^[a, b] Jinglei Cui,^[a, b] Tiansheng Deng,^[a] Xiaojing Cui,^[a] Guoqiang Ding,^[c]
Yulei Zhu,^{*[a, c]} and Yongwang Li^[a, c]

cctc_201402834_sm_miscellaneous_information.pdf

Table of Contents

1. Materials and Methods

2. Experiments

3. Results and discussion

4. The solubility of H₂ in different solvents

5. ¹HMR and ¹³CMNR of GVL

6. Mass spectrum of GVL

7. The effect of temperature on the hydrogenation reaction

8. Reusability study of Ru/TiO₂ catalyst

9. The effect of agitation rate on the conversion of LA

10. The typical GC chart of hydrogenation of LA to GVL

1. Materials

Levulinic acid (LA, 98%) and D₂O (99.9%) were purchased from Aladdin; methanol, ethanol, 1, 4-dioxane and γ -valerolactone (GVL, 98%) were purchased from Sinopharm Chemical Reagent Co., Ltd.. All the above agents were utilized without further purification. RuCl₃·3H₂O, γ -Al₂O₃, SiO₂, ZrO₂, and TiO₂ (P25 Degussa) were purchased from Sinopharm Chemical Reagent Co., Ltd.; Organic solvent-water mixtures were obtained by diluting 1 g deionized water with 9 g alcohols or 1,4-dioxane.

2. Experiments

2.1 The computational formula

The conversion of LA and the selectivity of the products (GVL) were quantified according to the following equations:

$$\text{Conversion} = \frac{\text{moles of LA(inlet)} - \text{moles of LA(outlet)}}{\text{moles of LA(inlet)}} \times 100\%$$

$$\text{Selectivity} = \frac{\text{moles of one product}}{\text{moles of all products}} \times 100\%$$

Turnover frequency (TOF) was calculated on the basis of surface Ru atoms, which is estimated with the total loadings of Ru.

$$\text{TOF} = \frac{\text{number of LA molecular converted}}{(\text{number of surface Ru atoms})(\text{reaction time,h})}$$

2.2 Catalyst characterization

2.2.1 X-ray diffraction (XRD) measurements Figure S2.

Powder X-ray diffraction (XRD) patterns were obtained on a D2/max-RA X-ray diffractometer (Bruker, Germany), with Cu K α radiation at 30 kV and 10 mA. The X-ray patterns were recorded in 2 θ values ranging from 5° to 80° with a scanning speed of 4 °/min.

2.2.2 Transmission electron microscope (TEM) Figure S3.

TEM measurements were performed with a field-emission transmission electron microscopy (FETEM, JEM-2011F) operating at 200 kV voltages. The reduced samples were suspended in ethanol with an ultrasonic dispersion for 30 min and deposited on copper grids coated with amorphous carbon films.

2.2.3 Temperature-programmed reduction (TPR) FigureS4.

Hydrogen temperature-programmed reduction (H₂-TPR) experiments were carried out on a micro automatic chemical adsorption instrument TP5080 with a TCD detector. Before the measurement, 20 mg catalyst (20-40 mesh) was loaded to a fixed-bed quartz microreactor (i.d.=4 mm) and pretreated in an N₂ flow of 30mL min⁻¹ at 200 °C for 0.5 h. After being cooled at the same atmosphere to room temperature (RT), the pretreated sample was exposed to a flow (30 mL/min) of 10 vol% H₂/N₂ mixture and heated from RT to 630 °C at a ramp of 10 °C /min.

2.2.4 ¹H and ¹³C nuclear magnetic resonance (¹HNMR and ¹³CNMR) Figure S5.

Liquid-state NMR experiments were performed on a Bruker AVANCE III 400 MHz spectrometer operating at 400-MHz ¹H and 100-MHz ¹³C frequencies.

2.2.5 Gas chromatograph-Mass spectrometer (GC-MS) Figure S6.

The liquid product was collected and analyzed by an Agilent GC-MS (6890 series GC with a 5973 MS detector) equipped with DB-WAX capillary(30 m×0.32 μm×0.5 μm) by the external standard method. Identification of the products was achieved with a spectral library (NIST MS Search 2005).

3. Results and discussion

Table S1 the TOF values of the Ru-based catalyst under 70°C

Entry	catalyst	LA con. %	TOF/ h ⁻¹	t/ min	T/ °C
1	Ru/Al ₂ O ₃	7.3	1275	15	70
2	Ru/SiO ₂	19.1	3330	15	70
3	Ru/ZrO ₂	21.6	3773	15	70
4	Ru/TiO ₂	44.0	7676	15	70

Reaction conditions: LA (5 g, 43.1mmol), 10 g water; H₂ (4 MPa); Ru (1 wt%)/support (0.1 g, 0.0099 mmol of Ru)

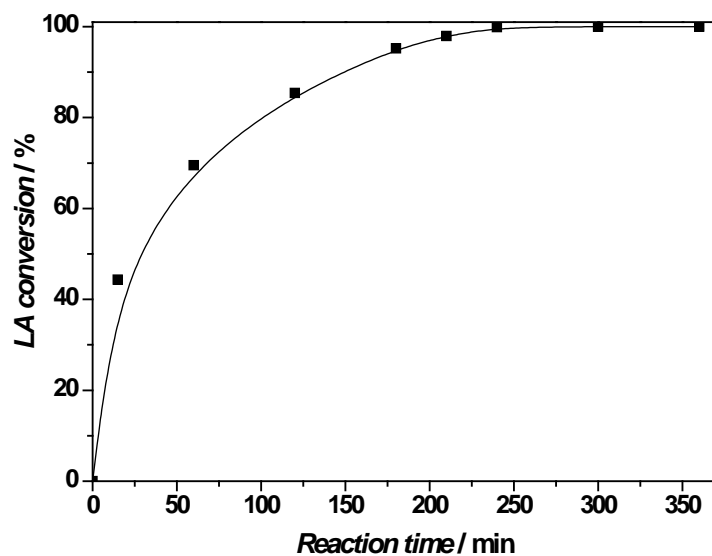


Figure S1 the kinetics profiles of LA hydrogenation to GVL

Reaction conditions: LA (5 g, 43.1mmol), 10 g water; H₂ (4 MPa); Ru (1 wt%)/TiO₂ (0.1 g, 0.0099 mmol of Ru) 70 °C

3.1 XRD patterns of Ru-based catalysts

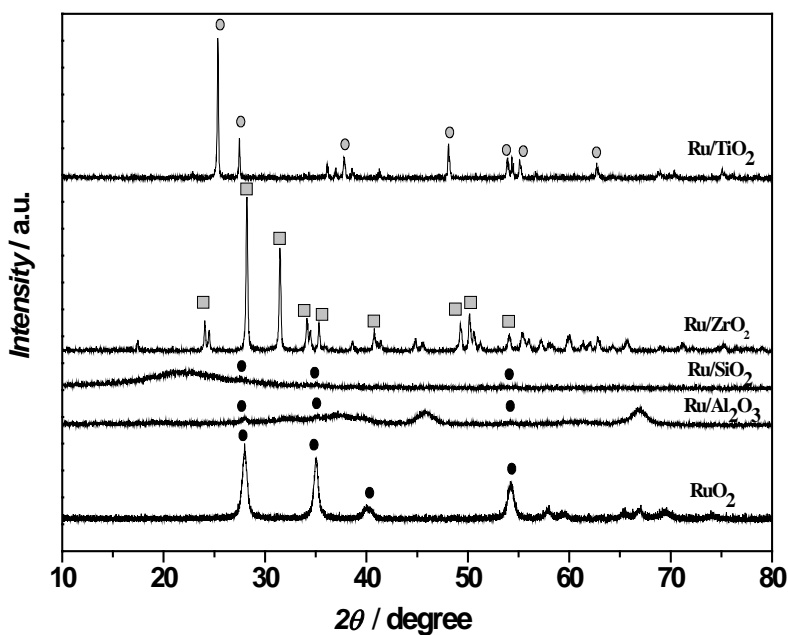


Figure S2. (a) XRD patterns of Ru-based catalysts with different supports and the patterns of pure RuO₂ (● RuO₂ ○ TiO₂ ■ ZrO₂)

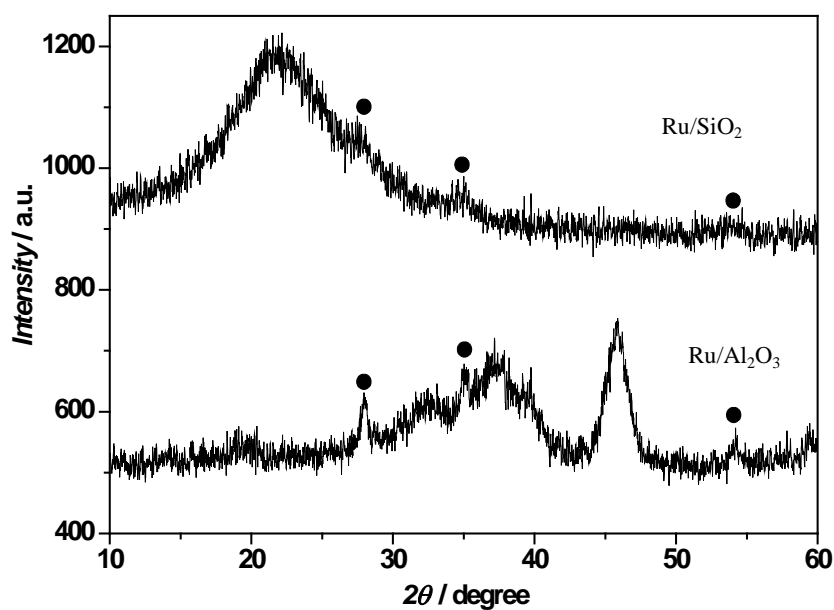


Figure S2. (b) XRD patterns of Ru/SiO₂ and Ru/Al₂O₃ (● RuO₂)

The XRD patterns of as-prepared Ru-based catalysts loaded on the different supports were displayed in Figure S2 (a). The diffraction peaks at around 28.0°, 35.2°, 37.3°, 40.3°, 54.4° are assigned to RuO₂ phase.^[1] The diffraction peaks represented anatase ($2\theta = 25.5^\circ, 38.1^\circ, 48.2^\circ, \text{ and } 54^\circ$) and rutile ($2\theta = 27.6^\circ \text{ and } 36.3^\circ$).^[2] The

diffraction peaks at 34.3° , 50.2° and 60.1° are associated with the tetragonal- ZrO_2 . Other diffraction peaks (24.1° , 28.3° , 31.6° and 40.8°) reveal the monoclinic- ZrO_2 .^[3] No diffraction peaks of RuO_2 appeared on the catalyst of Ru/ZrO_2 or Ru/TiO_2 . As can be seen in Figure S2 (b) some diffraction peaks of RuO_2 on the supports of Al_2O_3 or SiO_2 were detected.

3.2 TEM image of Ru-based catalyst

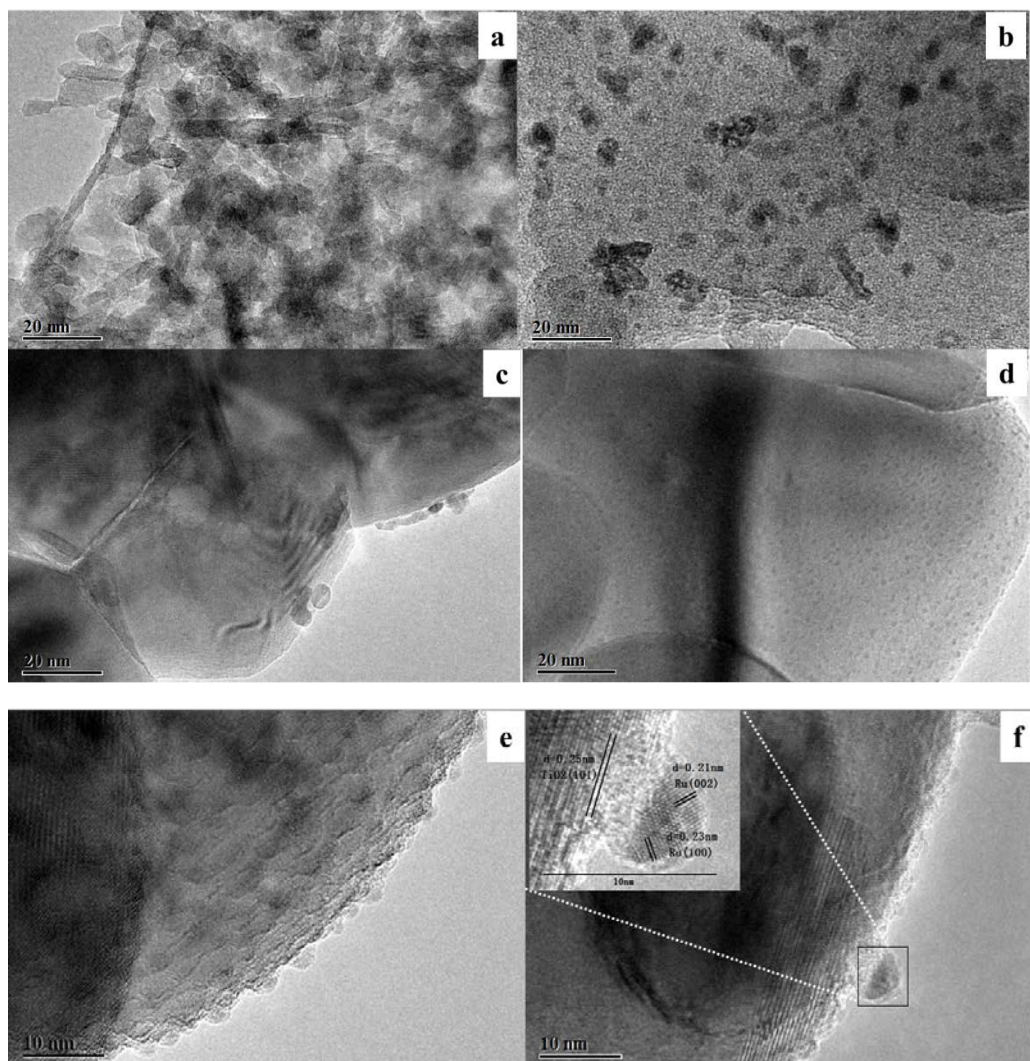


Figure S3. TEM image of supported catalyst of Ru/metal oxide after reduction (a) Ru/Al₂O₃ (b) Ru/SiO₂ (c) Ru/ZrO₂ (d) Ru/TiO₂, (e, f) HRTEM image of supported catalyst of Ru/TiO₂

3.3 TPR profiles of the supported Ru catalysts

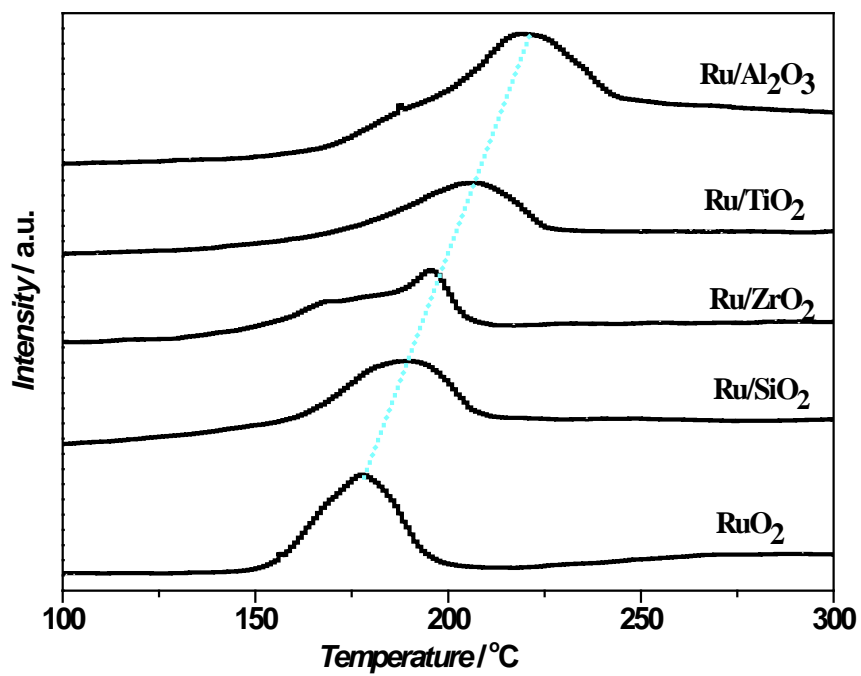


Figure S4. H₂-TPR profiles of the supported Ru catalysts

4. The solubility of H₂ in different solvents

The hydrogen solubility in the solvent, can be evaluated by the level of Henry constant of H₂ (K_H) that is calculated from Henry's law (the equation 1).

$$X_A = P_A / K_H \quad (1)$$

Where X_A represents the mole fraction of the solute gas in the liquid phase at the partial pressure of the solute gas at P_A

P_A - the equilibrium partial pressure

K_H -the Henry constant

According to equation (1), once the equilibrium pressure P_A is determined, the mole fraction of the solute gas in the liquid phase X_A is inversely proportional to the Henry constant K_H . Under the condition of room temperature and 0.3~2.0 MPa, the K_H value of hydrogen in water is 7500 MPa, while those in methanol and ethanol are 596 and 452 MPa respectively.^[4]

Table S2 The hydrogen solubility in the different solvents

Entry	solvent	P (MPa)			ΔP^a
		Pure H ₂ (P_1)	Solvent + LA (P_2)	Solvent+LA+H ₂ (P_3)	
1	none	5.55	-	-	-
2	water	-	0.12	5.50	0.17
3	1,4-dioxane	-	0.10	5.30	0.35
4	methanol	-	0.68	5.75	0.48
5	ethanol	-	0.50	5.45	0.60

Conditions: 130 °C, 4 MPa H₂ (Room temperature), 10 g of solvent, 5 g of LA, balance time =20 min; a: $\Delta P = P_1 + P_2 - P_3$.

At present, experimental results about hydrogen solubility in different solvents that are helpful to validate the aforementioned equation are scarce. However, a feasible comparison can be made for LA hydrogenation to GVL using the data measured by ΔP as shown in Table S2. In comparison with other organic solvent system, a minimum ΔP is seen in water system which confirmed that the lowest hydrogen solubility in water.

5. ^1H NMR and ^{13}C NMR of GVL

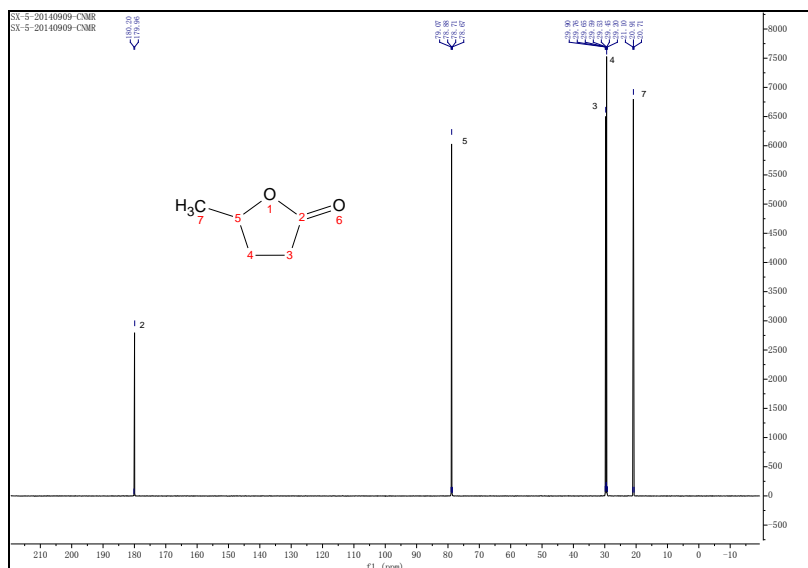


Figure S5. (a) The ^{13}C NMR spectroscopy of GVL standard sample
 ^{13}C NMR (101 MHz, D_2O) δ 179.96 (s), 79.38 – 78.53 (m), 30.97 – 29.46 (m), 29.32 (d, $J = 25.3$ Hz), 21.01 (d, $J = 18.6$ Hz), 20.71 (s).

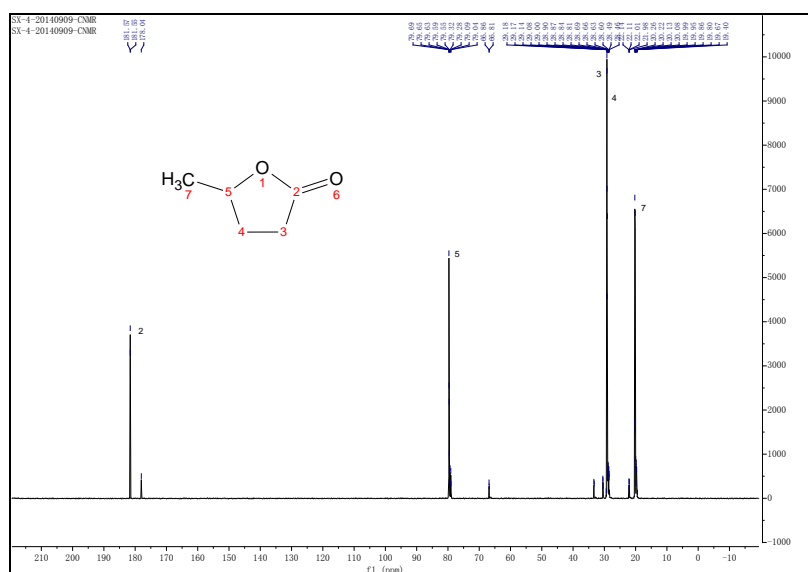


Figure S5. (b) The ^{13}C NMR spectroscopy of GVL produced from the hydrogenation of LA in the solvent of D_2O
 ^{13}C NMR (101 MHz, D_2O) δ 181.56 (d, $J = 1.6$ Hz), 178.04 (s), 79.79 – 79.23 (m), 79.07 (d, $J = 4.5$ Hz), 66.84 (d, $J = 4.9$ Hz), 33.29 (d, $J = 12.0$ Hz), 30.58 – 30.13 (m), 29.35 (d, $J = 9.5$ Hz), 29.28 – 28.05 (m), 22.06 (dd, $J = 13.2, 2.9$ Hz), 20.36 – 19.13 (m).

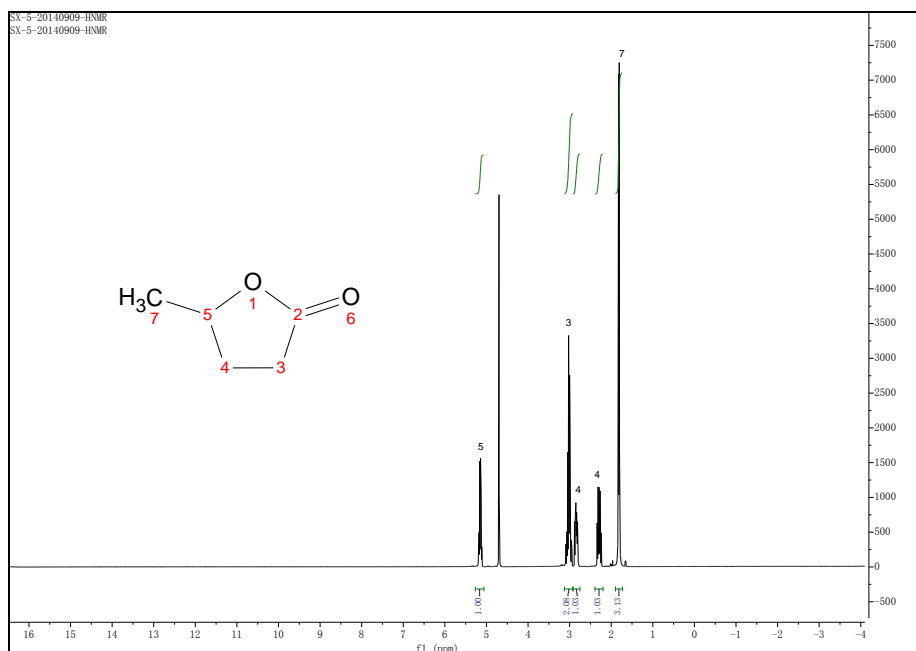


Figure S5. (c) The ^1H NMR spectroscopy of GVL standard sample
 ^1H NMR (400 MHz, D_2O) δ 5.24 – 5.06 (m, 1H), 3.11 – 2.90 (m, 2H), 2.87 – 2.75 (m, 1H), 2.29 (dtd, J = 12.6, 9.3, 8.0 Hz, 1H), 1.82 (d, J = 6.4 Hz, 3H).

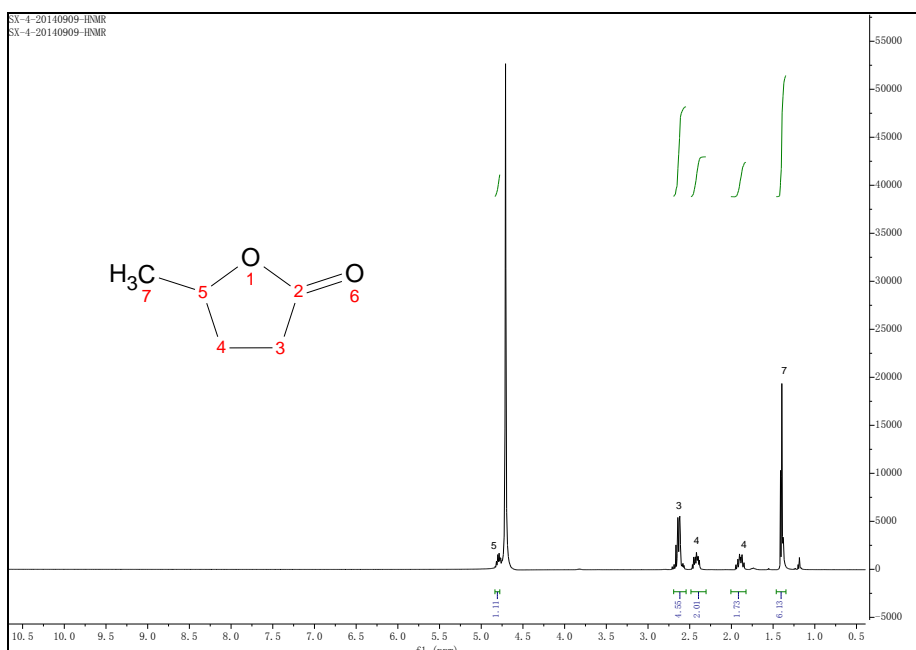


Figure S5. (d) The ^1H NMR spectroscopy of GVL produced from the hydrogenation of LA in the solvent of D_2O
 ^1H NMR (400 MHz, D_2O) δ 4.86 – 4.66 (m, 197H), 4.41 (s, 9H), 2.87 – 2.52 (m, 51H), 2.52 – 2.32 (m, 22H), 1.97 – 1.81 (m, 19H), 1.81 – 1.62 (m, 2H), 1.59 – 1.29 (m, 69H), 1.29 – 1.11 (m, 3H).

Compared with the ^{13}C NMR spectroscopy of GVL standard sample, ^{13}C NMR spectroscopy of GVL produced from the hydrogenation of LA in the solvent of D_2O yielded many split peaks (as can be seen the C5, C3, C4 and C7 in Figure S5 a and b), which implied that a part of H were on these carbons or on the adjacent carbons. Generally, in ^1H NMR, the ratio of the integral value of H peak is approximately equivalent to the ratio of the number of H atoms on each C atom. The ratio of integral value (C5: C3: C4: C7=1.11:4.55:3.73:6.13=0.488:2:1.64:2.69) in GVL produced from the hydrogenation of LA in the solvent of D_2O changed significantly by comparison to the ratio of integral value (C5: C3: C4: C7=1.0:2.08:2.06:3.13) in standard GVL sample (Figure S5 c and d), indicating that some of H was replaced by D in the hydrogenation process. Particularly, the D on C5 came from D_2O via hydrogenation of the C=O group of LA.

6. Mass spectrum of GVL

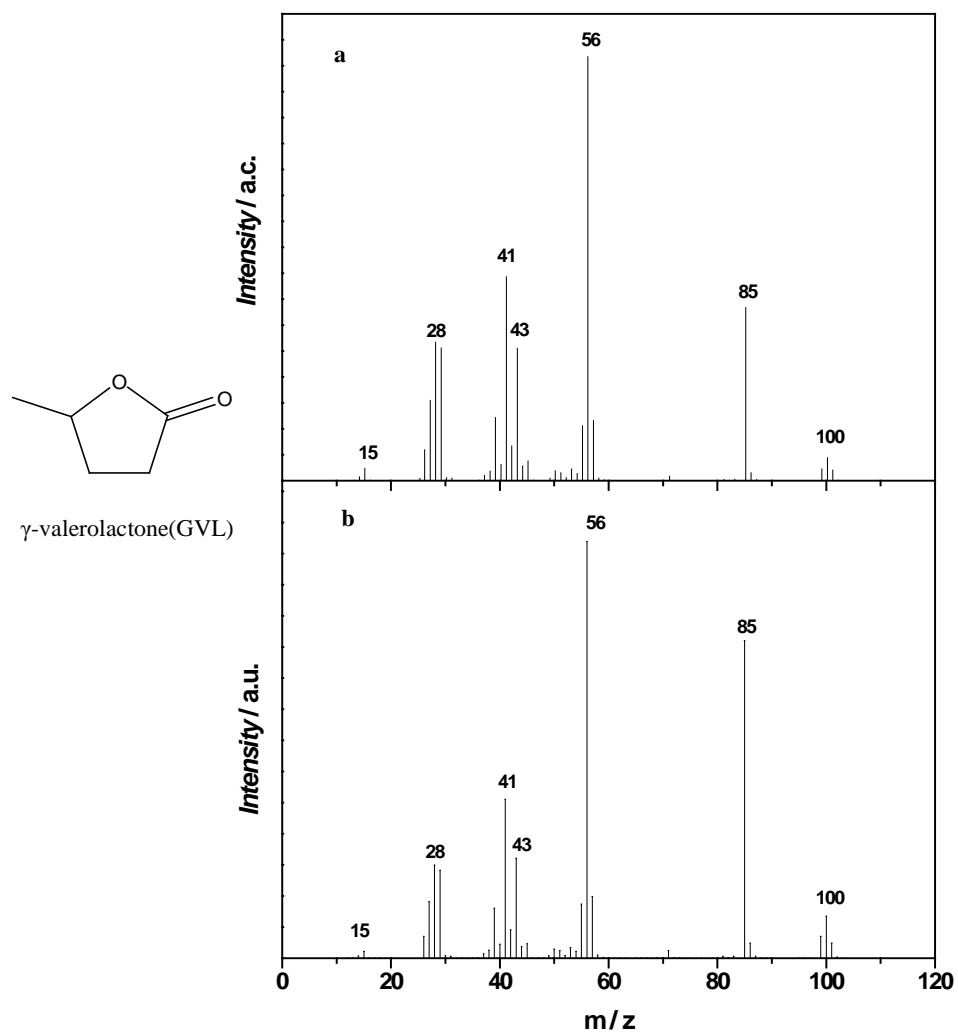


Figure S6. (a) The Mass spectrum of GVL standard sample (b) the Mass spectrum of GVL after mixing with D_2O

Compared with the Mass spectrum of GVL standard sample, it can be observed that there is no change for the m/z ratio of GVL produced from mixing with D_2O , implying that no D atom in GVL.

7. The effect of the temperature on the hydrogenation reaction

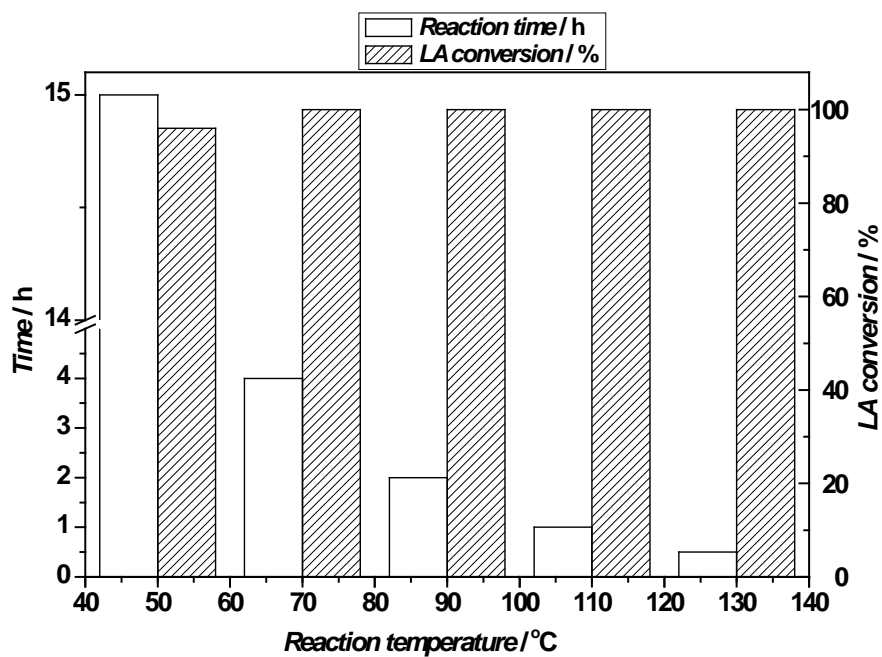


Figure S7. Influence of the temperature on the conversion of LA and the reaction time. Reaction conditions: LA (5 g, 43.1mmol), 10 g water; H₂ (4 MPa); Ru (1 wt%)/TiO₂ (0.1 g, 0.0099 mmol of Ru)

8. Reusability study of Ru/TiO₂ catalyst

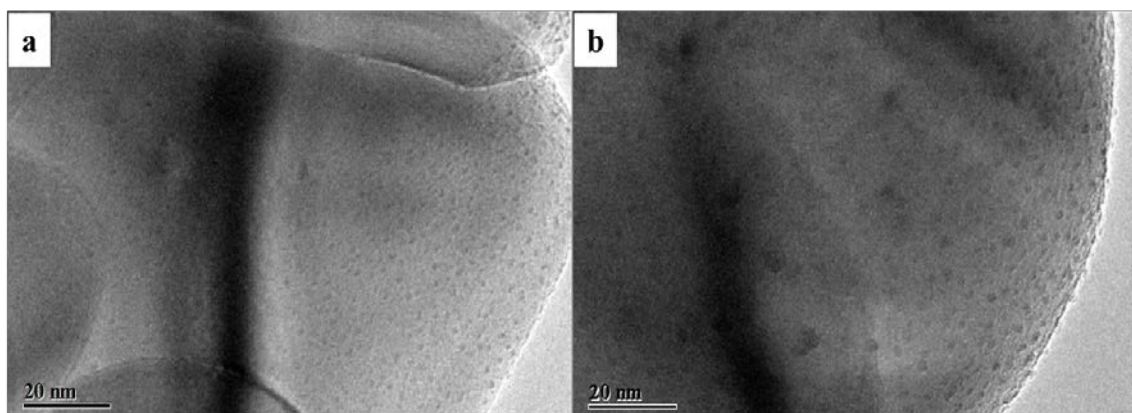


Figure S8. TEM image of supported catalyst of Ru/TiO₂ (a) fresh catalyst (b) catalyst spent for seven runs

9. The effect of agitation rate on the conversion of LA

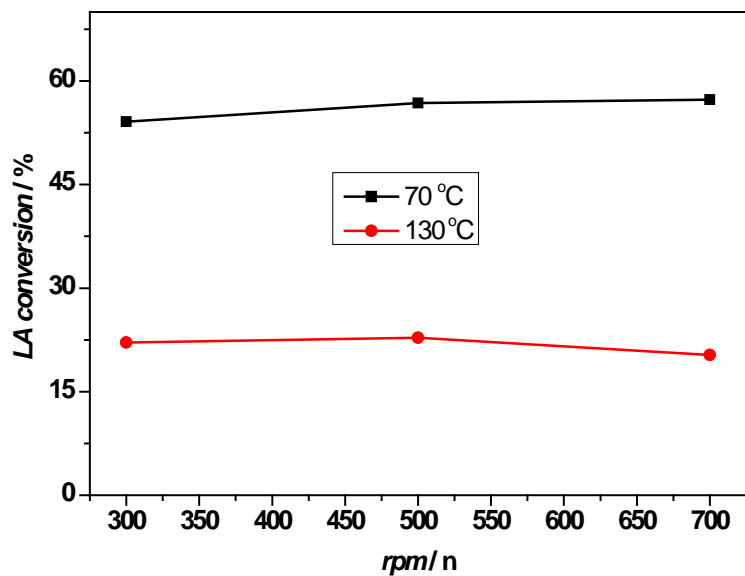


Figure S9. Conversion of LA at different agitation rates over 1wt% Ru/TiO₂
Reaction conditions: LA 5 g, water 10 g, H₂ 4 MPa, a) catalyst 0.1 g, 70 °C, t=1 h; b) catalyst 30 mg, 130 °C, t=30 min.

10. The typical GC chart of hydrogenation of LA to GVL

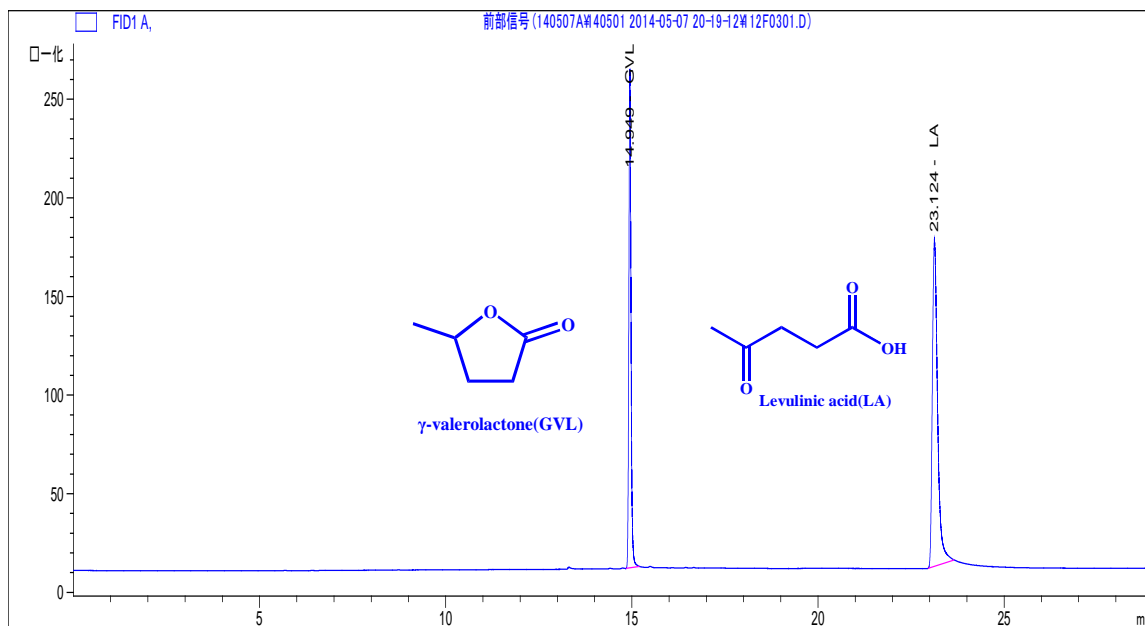


Figure S10. The typical GC chart of hydrogenation of LA to GVL

References

- [1] K. V. R. Chary, C. S. Srikanth and V. Venkat Rao, *Catal. Commun.* **2009**, 10,459-463.
- [2] T. W. Omotoso, S. Y. Boonyasuwat and S. P. Crossley, *Green Chem.* **2014**, 16, 645-652.
- [3] J. L. Bi, Y. Y. Hong, C. C. Lee., C. T. Yeh and C. B. Wang, *Catal. Toda*, **2007**,129, 322-329
- [4] M.G. Al-Shaal, W. R. H. Wright, R. Palkovits, *Green Chem.* **2012**, 14, 1260-1263